

Supporting Information

Mechanism of aggregate formation in simplified industrial silica styrene-butadiene nanocomposites: effect of chain mass and grafting on rheology and structure

Guilhem P. Baeza, Anne-Caroline Genix,* Christophe Degrandcourt, Jérémie Gummel, Marc Couty, and Julian Oberdisse

This document gives supplementary information on the determination of the volume fraction of fractal branches used in the coupled SAXS-TEM model (section 1), on silica structure in the lowest mass nanocomposite sample (section 2), and on aggregate structure at constant chain mass and %D3 (section 3).

1. Transmission electron microscopy (TEM)

The microstructure of nanocomposites with different molar mass has been measured by TEM and is shown in Figure S1. Image analysis of these TEM pictures allow for the determination of the volume fraction of fractal branches, Φ_{fract} , as indicated in the caption. As can be seen in Figure S2, these values are in good agreement with the estimation of Φ_{fract} based on the nanocomposites with 140 kg/mol (see Ref. ¹ for details).

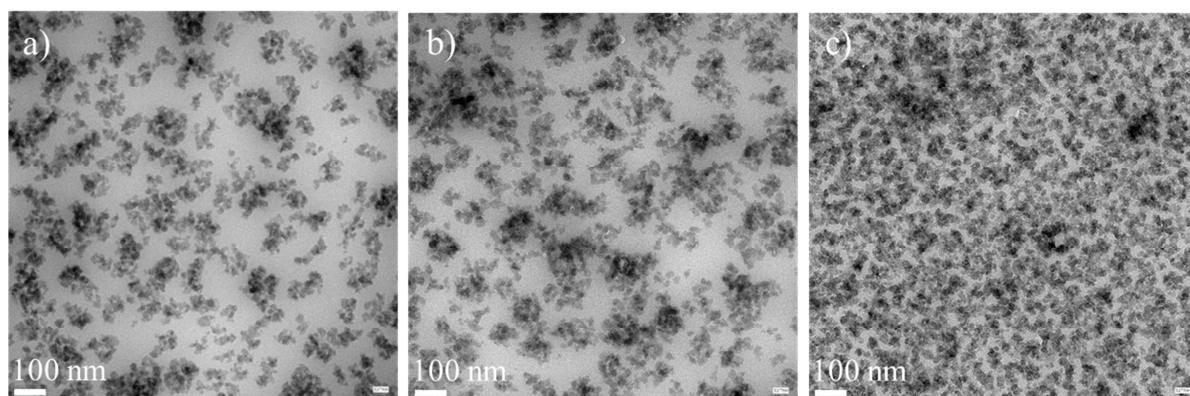


Figure S1. TEM of silica SB nanocomposites with a) $\Phi_{\text{si}} = 9.5\%v - 50\%D3 - 280 \text{ kg/mol}$ leading to $\Phi_{\text{fract}} = 47.5\%$, b) $\Phi_{\text{si}} = 9.5\%v - 100\%D3 - 280 \text{ kg/mol}$ leading to $\Phi_{\text{fract}} = 49.5\%$, and c) $\Phi_{\text{si}} = 18.8\%v - 100\%D3 - 40 \text{ kg/mol}$ leading to $\Phi_{\text{fract}} = 75.5\%$.

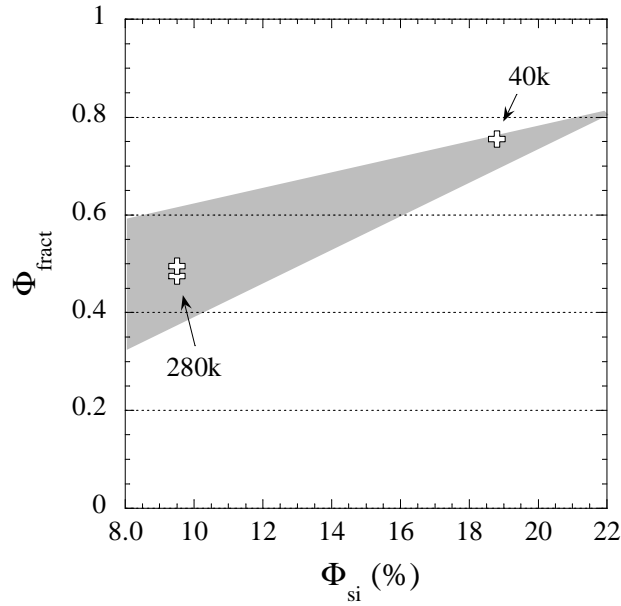


Figure S2. Evolution of the volume fraction of fractal branches as a function of the silica volume fraction. The grey triangular area has been obtained from quantitative analysis of the TEM pictures of nanocomposites with 140 kg/mol (see Appendix of Ref. ¹).

2. Silica structure without fragmentation

We focus here on the 10.4%v silica sample with the 40 kg/mol chains, which presents the same silica structure as the original silica powder. The Kratky presentation of the X-ray scattering data is shown in Figure S3 with a description in terms of two log-normal contributions (one for the primary silica nanoparticles at high q and another one for the aggregates). The log-normal position parameters were kept fixed to the same value as in Ref. ² for the silica bead $q_{si} = (\pi/13.85 \text{ nm})$ and to $q_{agg} = \pi/R_{max} = (\pi/49.15 \text{ nm})$ for the aggregates.

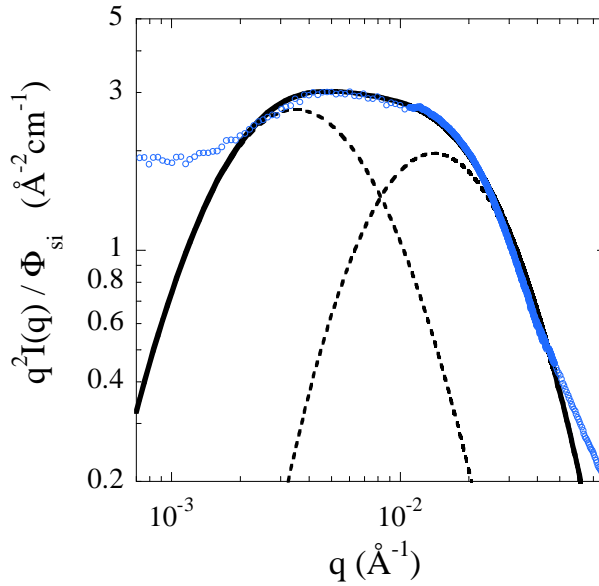


Figure S3. Kratky representation of the reduced scattered intensity $q^2 I(q)/\Phi_{si}$ for the nanocomposite with $\Phi_{si} = 10.4\%v - 50\%D3 - 40 \text{ kg/mol}$. Data are described by the sum (line) of two log-normal functions (dotted lines) with the q -position fixed.

3. Aggregate structure at constant chain mass and same %D3

We may recall here previous results obtained by varying the silica volume fraction in nanocomposites with 140 kg/mol and 50% of functionalized chains². In this case, we found that aggregates approximately conserve their average mass (N_{agg}), but contract slightly (small reduction of R_{agg}), leading to an increase of their compacity from 31 to 38%. However, as illustrated in Figure S4, changing the silica volume fraction at constant chain mass and %D3 leads to a simultaneous decrease of the grafting density ρ_{D3} . Thus the silica concentration line studied in Ref.² corresponds to a tilted line on the ρ_{D3} -diagram shown in Figure 7, where the extreme points of the line are marked, and not to a vertical line at fixed ρ_{D3} , where a strong decrease of both N_{agg} and R_{agg} with Φ_{si} could be expected.

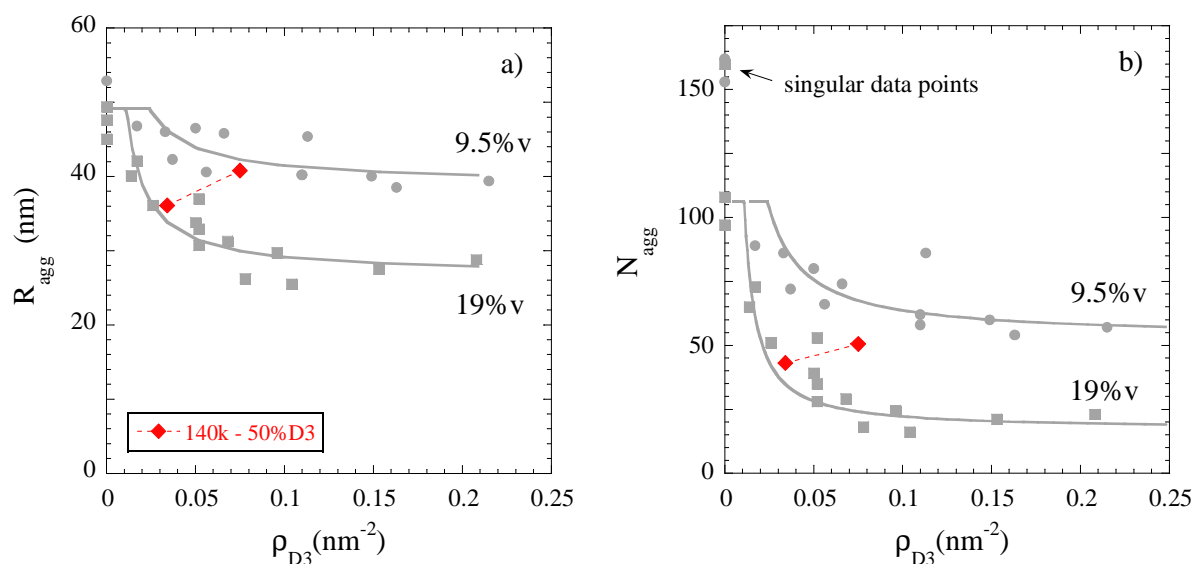


Figure S4. Average aggregate radius R_{agg} (a) and average aggregation number N_{agg} (b) as a function of ρ_{D3} , for all data regrouped in subsets at ca. 9.5% v (circles) and 19% v (squares) silica fractions. See details in the main manuscript for the fit functions (lines). Results for samples with 140 kg/mol and 50% D3 are highlighted by red diamonds.

References

- (1) Baeza, G. P.; Genix, A. C.; Degrandcourt, C.; Petitjean, L.; Gummel, J.; Schweins, R.; Couty, M.; Oberdisse, J. *Macromolecules* **2013**, *46* (16), 6388–6394.
- (2) Baeza, G. P.; Genix, A. C.; Degrandcourt, C.; Petitjean, L.; Gummel, J.; Couty, M.; Oberdisse, J. *Macromolecules* **2013**, *46* (1), 317-329.